

# THE MEVALONATE-INDEPENDENT PATHWAY TO ISOPRENOID COMPOUNDS: DISCOVERY, ELUCIDATION, AND REACTION MECHANISMS

Reported by Leigh Anne Furgerson

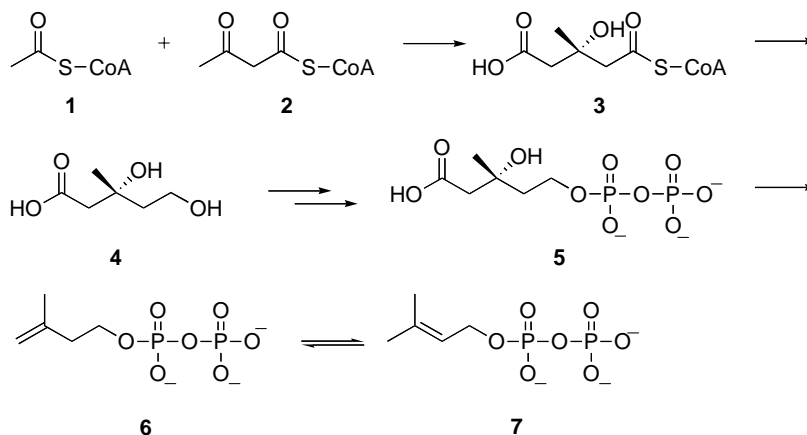
February 13, 2006

## INTRODUCTION

Isoprenoids comprise one of the largest and most structurally diverse classes of natural products, with more than 35,000 reported members.<sup>1</sup> They have numerous biological functions including electron transport, transcriptional regulation, and lipid membrane biosynthesis, as well as applications in the biotechnological production of pharmaceuticals, pigments, flavors, and agrochemicals.<sup>2,3</sup> The universal precursors to isoprenoids are the C<sub>5</sub> compounds isopentenyl diphosphate (IPP, **6**) and its isomer dimethylallyl diphosphate (DMAPP, **7**). Over half a century ago, work done by Bloch, Cornforth, and Lynen showed that these precursors are biosynthesized by the mevalonate pathway (Scheme 1).<sup>4</sup> For many years following its documentation, the mevalonate pathway, named for intermediate **4**, was thought to be the only route to isoprenoid precursors, and that knowledge was used to create the statin drugs that successfully treat hypercholesterolemia.<sup>5</sup>

In the early 1990s, isotope labeling experiments designed to determine the origin of carbon atoms in terpenoids and ubiquinones in resulted in the discovery of a novel, mevalonate-independent metabolic pathway.<sup>6,7</sup> This work was performed independently by Rohmer, with bacteria,<sup>6</sup> and Arigoni, with ginkgolide seedlings,<sup>7</sup> and led to the documentation of the 2C-methyl-D-erythritol, or MEP, pathway of isoprenoid biosynthesis (Scheme 2). To date, five of the seven reactions composing this pathway have been fully characterized, including the enzyme mechanism. The final two steps leading directly to IPP (**6**) and DMAPP (**7**) remain to be fully elucidated. This seminar will review the discovery of the mevalonate-independent pathway and also will discuss the elucidation of its reaction mechanisms as they are presently understood.

Scheme 1. Mevalonate Pathway

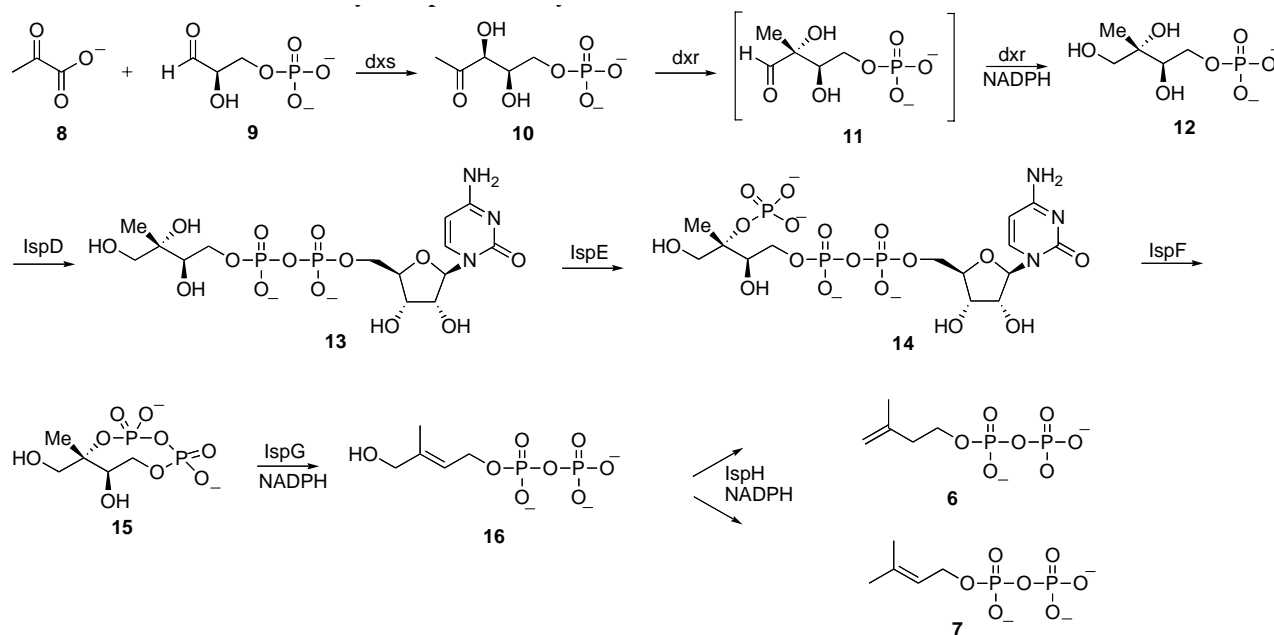


## DISCOVERY

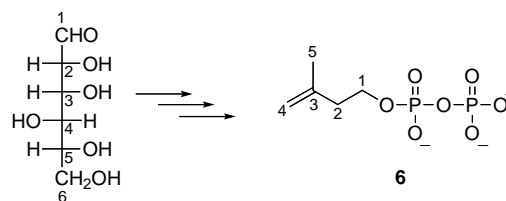
The first indications of a novel isoprenoid biosynthetic pathway came from the results of isotopic labeling studies done by Rohmer and co-workers in the late 1980s.<sup>8</sup> In these studies, the incorporation

of [1-<sup>13</sup>C] and [2-<sup>13</sup>C]acetate into pentacyclic triterpenoids was investigated. The observed labeling patterns differed significantly from the isotopic distributions expected based on biosynthesis from the mevalonate pathway. A follow-up experiment tracking [5-<sup>13</sup>C]glucose incorporation into *Zymomonas mobilis* hopanoids also resulted in unexpected labeling patterns.<sup>9</sup> Although the results were incompatible with the traditional mevalonate pathway, there was not enough evidence at that time to propose an alternative.

**Scheme 2. Nonmevalonate Pathway for Isoprenoid Biosynthesis.**



The seminal experiments were reported in 1993, when Rohmer and co-workers followed four <sup>13</sup>C-labeled isoprenoid precursors through the metabolic pathways of four bacteria.<sup>6</sup> Each bacterial strain was grown on synthetic media containing only one carbon source, and the location of <sup>13</sup>C in resulting triterpenoids was analyzed by <sup>13</sup>C NMR spectroscopy. The observed isotopic distributions were then traced back to IPP (Figure 1). C3 and C5 of IPP arise from glucose C2 or C5 and C3 or C6, respectively. The most likely precursor was considered to be a decarboxylated pyruvate, arising either from cleavage of 2-oxo-3-deoxy-6-phospho-gluconate or from glyceraldehyde-3-phosphate metabolism.



% IPP Isotopic Enrichment

	C-1	C-2	C-3	C-4	C-5
C-1	-	-	-	-	-
C-2	-	-	50	-	-
C-3	-	-	-	-	50
C-5	100	50	-	-	-
C-6	100	-	-	-	50

**Figure 1.** Isotopic labeling pattern of IPP from <sup>13</sup>C-labeled glucose. The percent isotopic enrichment refers to the amount of observed <sup>13</sup>C enrichment present at that location.

IPP carbons 1, 2, and 4, derived from glucose C-6, C-5, and C-4, respectively and based on double-labelling experiments, were introduced simultaneously. The labeling pattern required the pyruvate precursor to be inserted between two carbons of a C<sub>3</sub> fragment. This implicated the involvement of a dihydroxyacetone derivative such as glyceraldehyde-3-phosphate (**9**). As each of the above-mentioned conditions was inconsistent with the mevalonate pathway, a novel biosynthetic route was proposed.<sup>6</sup> Similarly, Arigoni and co-workers independently proposed a mevalonate-independent pathway based on isotopic labeling experiments with [U-<sup>13</sup>C<sub>6</sub>]glucose and ginkgolides in seedlings of the *Ginkgo biloba* tree.<sup>7</sup> The proposed pathway was incomplete with many questions marks, but served as a template for future research. Since then, the mechanisms of five steps have been characterized and the remaining three are in the beginning phases.

## ENZYMES-CATALYZED REACTIONS

### 1-Deoxy-D-xylulose-5-phosphate Synthase (dxs)

1-Deoxy-D-xylulose-5-phosphate synthase catalyzes the formation of 1-deoxy-D-xylulose-5-phosphate (DXP, **10**) by a thiamin-dependent aldol condensation between pyruvate (**8**) and D-glyceraldehyde-3-phosphate (**9**) (Figure 2). The stereochemistry of the product results from nucleophilic attack on the *si* face of the aldehyde.<sup>10</sup> This first step of the nonmevalonate pathway is not considered the first committed step since DXP is also the precursor to thiamin and pyridoxal.

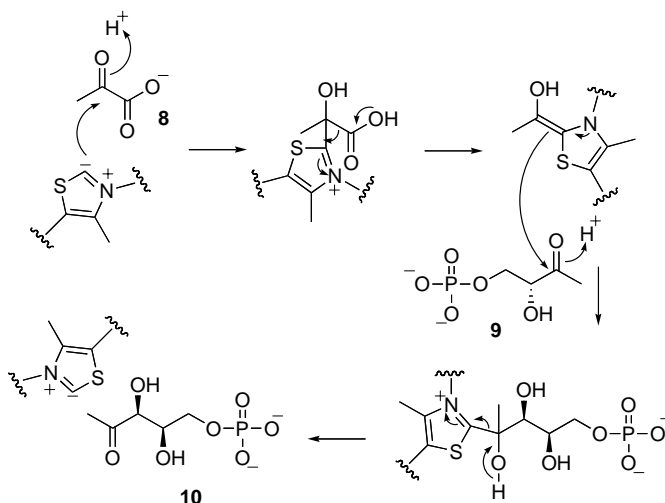
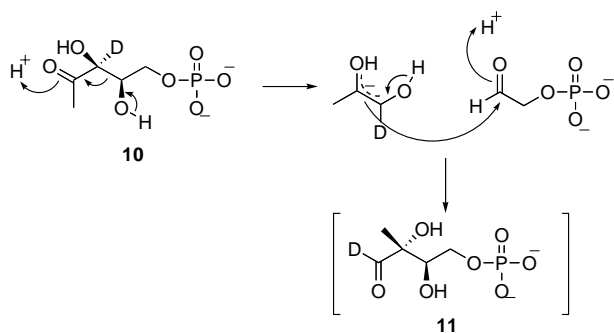


Figure 2. Mechanism of 1-deoxy-D-xylulose-5-phosphate synthase.

### 1-Deoxy-D-xylulose-5-phosphate Reductoisomerase (DXR, IspC)

The second enzyme of the MEP pathway catalyzes the reductive transformation of DXP to 2C-methyl-D-erythritol-4-phosphate (MEP) (**12**). Conversion to MEP is considered the first committed step of the nonmevalonate pathway. The first step of the DXR-catalyzed reaction is a skeletal rearrangement of DXP (**10**) to the hypothetical aldehyde intermediate **11** (Scheme 2). Subsequent reduction of **11** affords 2C-methyl-D-erythritol-4-phosphate, or MEP. While no direct evidence exists to confirm the presence of **11**, enzymatic assays with synthetic **11** and DXR resulted in formation of MEP.<sup>11</sup> Thus it is thought the aldehyde is in fact an intermediate but is not released from the enzyme active site. Of the two proposed mechanisms for the rearrangement, the majority of supporting evidence is consistent with



**Figure 3.** Proposed retroaldol mechanism of 1-deoxy-D-xylulose 5-phosphate reductoisomerase.

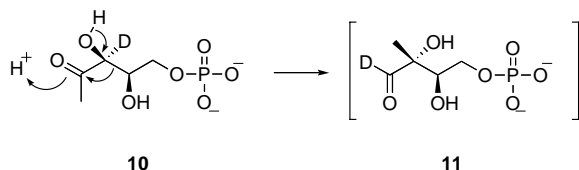


**Figure 4.**  $\alpha$ -Ketol rearrangement mechanism of DXR.

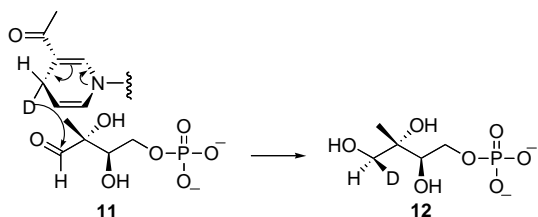


**Figure 5.** Stereochemical course of the dxr reduction step. The reduction of aldehyde **11** proceeds via hydride transfer from NADPH. Experiments performed with  $[3\text{-}^2\text{H}]\text{DXP}$  and  $(4S)\text{-}[^2\text{H}]\text{NADPH}$  show reduction occurs by transfer of the  $4S$ -hydride from NADPH to the *re* face of the aldehyde (Figure 5).<sup>13</sup> Thus the pro-R hydrogen from NADPH and the pro-S from DXP.

a retroaldol reaction followed by a forward aldol reaction (Figure 3). This mechanism was supported by the results of kinetic studies using a 1-fluorinated analogue of DXP as the substrate, which found that the rearrangement was accelerated with the fluorinated substrate.<sup>12</sup> This is both evidence for the retroaldol mechanism and against the other proposed mechanism (Figure 4). The second mechanism is an  $\alpha$ -ketol rearrangement requiring both protonation of the ketone and carbenium ion formation, both of which are disfavored by the presence of a fluorine atom. Fluoro substitution is expected to accelerate the retroaldol mechanism due to stabilization of the intermediary enolate. The reduction of aldehyde **11** proceeds via hydride transfer from NADPH. Experiments performed with  $[3\text{-}^2\text{H}]\text{DXP}$  and  $(4S)\text{-}[^2\text{H}]\text{NADPH}$  show reduction occurs by transfer of the  $4S$ -hydride

#### 4-Diphosphocytidyl-2C-methyl-D-erythritol Synthase (IspD)

The third enzyme of the nonmevalonate pathway catalyzes the cytidine triphosphate (CTP) (**17**)-dependent transformation of MEP (**12**) to 4-diphosphocytidyl-2C-methyl-D-erythritol (CDP-ME) (**13**). An X-ray crystal structure of the enzyme bound with both  $\text{Mg}^{2+}$  and CDP-ME, and isotopic labeling studies, have provided evidence for the mechanism of this reaction (Figure 6).<sup>14</sup> The associative mechanism involves nucleophilic attack by the MEP phosphate on the  $\alpha$ -phosphate of CTP, resulting in pentacoordinate transition state **18**. Collapse of the transition state forms the two products, CDP-ME (**13**) and inorganic pyrophosphate. The large amount of negative charge in the active site is stabilized by the presence of two Lys (27 and 213) and two Arg (19 and 20) residues and a  $\text{Mg}^{2+}$  ion. Other residues important for enzyme activity are Asp106, Arg109, Thr165, and Thr140' which aid in MEP binding and orientation. Pulse-chase experiments using  $[2\text{-}^{14}\text{C}]\text{MEP}$  or  $[2\text{-}^{14}\text{C}]\text{CTP}$  established that substrate binding is ordered, with CTP binding first. It is thought that CTP binding induces a conformational change in the active site, allowing MEP to attain the proper orientation for attack.<sup>14</sup>

#### 4-Diphosphocytidyl-2C-methyl-D-erythritol Kinase (IspE)

The enzyme IspE catalyzes the single ATP-dependent step in the pathway. In this reaction, the  $\gamma$ -phosphoryl group of ATP is transferred to the tertiary C2 hydroxyl of CDP-ME forming 4-diphosphocytidyl-2C-methyl-D-erythritol-2-phosphate (CDP-ME2P) (**14**).<sup>15</sup> Experiments with <sup>13</sup>C- and <sup>14</sup>C-labeled CDP-ME first implicated the formation of CDP-ME2P as an intermediate in the pathway, and that it was later incorporated into carotenoids.<sup>16</sup>

A crystal structure of CDP-ME kinase in a ternary complex with CDP-ME and an ATP analog suggests the associative mechanism shown in Figure 7.<sup>15</sup> The phosphate transfer is facilitated by deprotonation of the C2 hydroxyl by Asp141 and also by stabilization of the pentavalent, highly negatively charged transition state by Lys10.

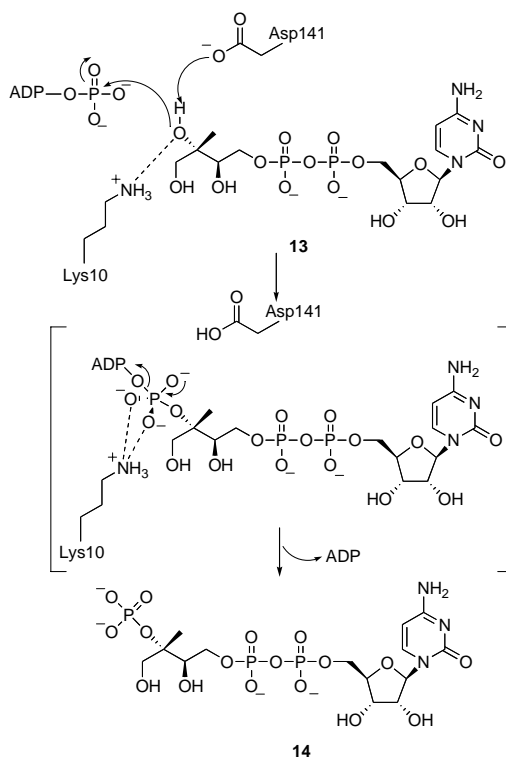


Figure 7. Mechanism of IspE catalyzed reaction.

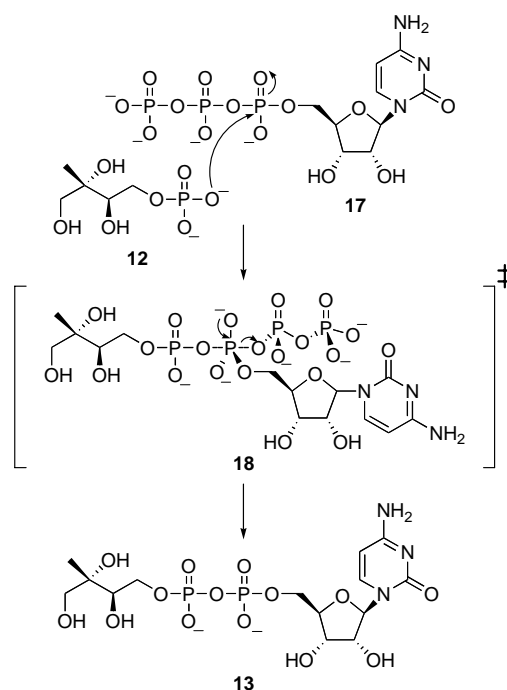
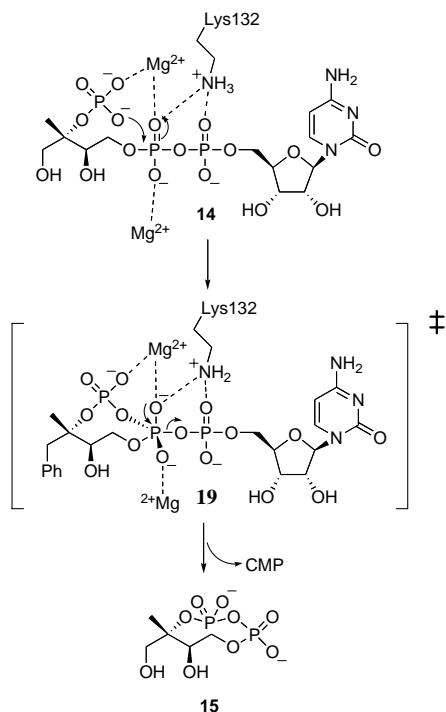


Figure 6. Mechanism of reaction catalyzed by IspD.

#### 2C-Methyl-D-erythritol 2,4-cyclodiphosphate Synthase (IspF)

The fifth reaction of the MEP pathway (Scheme 2) is the IspF-catalyzed formation of 2C-methyl-D-erythritol 2,4-cyclodiphosphate (MECDP) (**15**) from 4-diphosphocytidyl-2C-methyl-D-erythritol-2-phosphate (**14**). The reaction is divalent metal cation-dependent and proceeds by intramolecular nucleophilic attack of the 2-phosphate on the  $\beta$ -phosphate, releasing cytidine monophosphate (CMP) and MECDP (**15**) (Figure 8).<sup>16</sup> The magnesium ions contribute significantly to the enzyme activity by both stabilizing the highly negatively charged pentacoordinate transition state **19** and also by appropriately orienting the attacking phosphate. CDP-ME2P (**14**) non-enzymatically cyclizes to release CDP, so proper orientation by MECDP synthase is required for nucleophilic attack on the  $\beta$ -

phosphate.



**Figure 8.** Mechanism of the reaction catalyzed by IspF.

#### 4-Hydroxy-3-methyl-(2E)-butenyl Diphosphate Synthase (IspG)

IspG is the sixth enzyme in the sequence and is responsible for the reductive ring opening of MECDP to form 4-hydroxy-3-methyl-(2E)-butenyl diphosphate (HMB-PP, **16**). The existence of HMB-PP was first determined by NMR studies of cell extracts incubated with  $[U-^{13}C_5]$ 1-deoxy-D-xylulose and engineered to overexpress the first six enzymes of the nonmevalonate pathway.<sup>18</sup> Once HMB-PP was shown to be an intermediate in the pathway, and a precursor to IPP and DMAPP, mechanistic studies began. To date, more than one mechanism has been proposed but none are widely agreed upon.

The first studies showed that cell extract was capable of converting MECDP to HMB-PP, but little to no activity was observed with the purified enzyme. Since the reaction catalyzed by IspG is formally a reduction and UV-visible spectroscopy showed a shoulder at 410 nm, it was thought that cofactors would be necessary for activity, and many natural and artificial redox systems were tested as possible electron donors. Upon restoration of an iron-sulfur cluster with  $FeCl_3$  and  $Na_2S$  and implementation of an NADPH/flavodoxin/flavodoxin reductase system under anaerobic conditions, the enzyme was capable of performing the transformation.<sup>19</sup>

One proposed mechanism is shown in Figure 9, and involves an initial intramolecular attack of the 2-hydroxyl on C3, forming an epoxide intermediate and opening the diphosphate ring. The subsequent steps involve two single-electron reductions by an Fe-S cluster to yield the final unsaturated product. Formation of the epoxide intermediate is supported by the previously demonstrated ability of Fe-S complexes to deoxygenate epoxides to alkenes in the presence of a reducing agent.<sup>20</sup> However, computer modeling studies suggest that epoxide formation, in lieu of a tertiary carbocation, is thermodynamically unfavorable.<sup>21</sup>

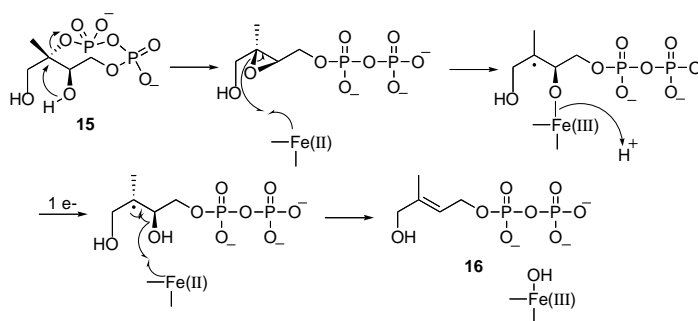


**Figure 9.** Hypothetical mechanism for the reaction catalyzed by IspG.

#### 4-Hydroxy-3-methyl-(2E)-butenyl diphosphate reductase (IspH)

IspH, the final enzyme of the nonmevalonate pathway, is responsible for converting HMB-PP (**16**) into both IPP (**6**) and DMAPP (**7**). This reaction is thought of as the biological equivalent of a Birch reduction of allylic alcohols, and the proposed mechanism is shown in Figure 10.<sup>22</sup> This enzyme is also dependent on an Fe-S cluster and NADPH/flavodoxin/flavodoxin reductase for activity. This suggests the reaction mechanism follows a radical pathway, although this is the sole evidence for the proposed mechanism. The hypothetical mechanism involves two single-electron transfers from the Fe-S cluster to HMB-PP to form transient carb-anion **19**, which is then followed by protonation from the *si* face. Based on <sup>13</sup>C NMR studies, the ratio of formation of IPP to DMAPP varies from 4-6:1 depending on the redox shuttle proteins used in experimentation.<sup>22</sup> The ratio of IPP to DMAPP at equilibrium is 1:3.1 and therefore the reaction catalyzed by IspH operates under kinetic control.

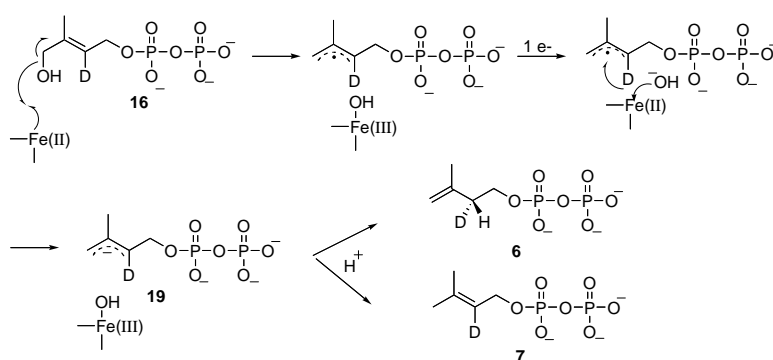


Figure 10. Hypothetical mechanism for the reaction catalyzed by IspH.

#### CONCLUSION

The significance of the discovery of a mevalonate-independent pathway to isoprenoid compounds has not yet been fully realized. All seven enzymes in the pathway represent new antimicrobial or parasitic drug targets for the pharmaceutical industry, as there are no known human homologs. The drug fosmidomycin is already showing potential as an anti-malarial drug in mice models, and has been shown to inhibit the second enzyme in the pathway, DXR.<sup>23</sup> As the crystal structures of these enzymes are solved to higher and higher resolution, a structure-based approach to inhibitor design can be applied to drug discovery, as in the case with fosmidomycin.

The distribution of the MEP pathway in different taxonomic kingdoms suggests the evolution of the two isoprenoid pathways. Based on gene searching of the fully sequenced genomes currently available, it appears as if archaeobacteria and early-branched eubacteria exclusively use the mevalonate pathway, while later eubacteria utilize the non-mevalonate pathway. Arigoni and co-workers determined that both pathways are utilized by plants, the non-mevalonate in chloroplasts and the

mevalonate in the cytosol.<sup>24</sup> It is widely accepted that chloroplasts originated by endocytosis of cyanobacteria, and thus the MEP pathway genes in plants are thought to have been imported into the nuclear genome in this way.

In order for scientists to better understand this new metabolic pathway, future research will concentrate on identifying the regulatory mechanisms involved. A crystal structure of IspF, the fifth enzyme in the sequence, shows the presence of farnesyl and geranyl diphosphate moieties bound to the enzyme, implicating a feedback loop method of regulation.<sup>2</sup> It is critical to understand these regulatory mechanisms of the MEP pathway in order to predict the most promising methods of inhibition for clinical applications. The non-mevalonate pathway clearly provides an area of exciting research for many years to come.

## REFERENCES

- (1) Rohdich, F.; Bacher, A.; Eisenreich, W. *Bioorg. Chem.* **2004**, *32*, 292-308.
- (2) Kemp, L. E.; Alpey, M. S.; Bond, C. S.; Ferguson, M. A. J.; Hecht, S.; Bacher, A.; Eisenreich, W.; Rohdich, F.; Hunter, W. N. *Acta Cryst.* **2005**, *D61*, 45-52.
- (3) Campos, N.; Rodriguez-Concepcion, M.; Seemann, M.; Rohmer, M.; Boronat, A. *FEBS Lett.* **2001**, *488*, 170-173.
- (4) a) Qureshi, N.; Porter, J. W. In *Biosynthesis of Isoprenoid Compounds*; Porter, J. W.; Spurgeon, S. L., Eds; Wiley; New York, NY, 1981; Vol. 1, pp 47-94. b) Bochar, D. A.; Friesen, J. A.; Stauffacher, C. V.; Rodwell, V. W. In *Comprehensive Natural Products: Isoprenoids Including Carotenoids and Steroids*; Barton, D.; Cane, D. E.; Meth-Cohn, O.; Nakanishi, K.; Pergamon; New York, 1999; Vol. 2, pp 16-44.
- (5) Rohdich, F.; Hecht, S.; Gartner, K.; Adam, P.; Krieger, C.; Amslinger, S.; Arigoni, D.; Bacher, A.; Eisenreich, W. *Proc. Natl. Acad. Sci.* **2002**, *99*, 1158-1163.
- (6) Rohmer, M.; Knani, M.; Simonin, P.; Sutter, B.; Sahm, H. *Biochem. J.* **1993**, *295*, 517-524.
- (7) Schwarz, M. K. *Terpen-Biosynthese in Ginkgo biloba: Eine Uberraschende Geschichte* **1994**, Thesis Nr. 10951, ETH Zurich, Schweiz.
- (8) Flesch, G.; Rohmer, M. *Eur. J. Biochem.* **1988**, *175*, 405-411.
- (9) Rohmer, M.; Sutter, B.; Sahm, H. *J. Chem. Soc., Chem. Commun.* **1989**, 1471-1472.
- (10) Rohmer, M.; Seemann, M.; Horbach, S.; Bringer-Meyer, S.; Sahm, H. *J. Am. Chem. Soc.* **1996**, *118*, 2564-2566.
- (11) Hoeffler, J. F.; Tritsch, D.; Grosdemange-Billiard, C.; Rohmer, M. *Eur. J. Biochem.* **2002**, *269*, 4446-4457.
- (12) Fox, D. T.; Poulter, C. D. *Biochemistry* **2005**, *44*, 8360-8368.
- (13) Proteau, P. J.; Woo, Y. H.; Williamson, R. T.; Phaosiri, C. *Org. Lett.* **1999**, *1* 921-923.
- (14) Richard, S. B.; Lillo, A. M.; Tetzlaff, C. N.; Bowman, M. E.; Noel, J. P.; Cane, D. E. *Biochemistry* **2004**, *43*, 12189-12197.
- (15) Miallau, L.; Alpey, M. S.; Kemp, L. E.; Leonard, G. A.; McSweeney, S. M.; Hecht, S.; Bacher, A.; Eisenreich, W.; Rohdich, F.; Hunter, W.N. *Proc. Natl. Acad. Sci.* **2003**, *100*, 9173-9178.
- (16) Luttggen, H.; Rohdich, F.; Herz, S.; Wungsintaweekul, J.; Hecht, S.; Schuhr, C. A.; Fellermeier, M.; Sagner, S.; Zenk, M. H.; Bacher, A.; Eisenreich, W. *Proc. Natl. Acad. Sci.* **2000**, *97*, 1062-1067.
- (17) Kishida, H.; Wada, T.; Unzai, S.; Kuzuyama, T.; Takagi, M.; Terada, T.; Shirouzu, M.; Yokoyama, S.; Tame, J. R. H.; Park, S. Y. *Acta Cryst.* **2003**, *D59*, 23-31.
- (18) Hecht, S.; Eisenreich, W.; Adam, P.; Amslinger, S.; Kis, K.; Bacher, A.; Arigoni, D.; Rohdich, F. *Proc. Natl. Acad. Sci.* **2001**, *98*, 14837-14842.
- (19) Seemann, M.; Tse Sum Bui, B.; Wolff, M.; Tritsch, D.; Campos, N.; Boronat, A.; Marquet, A.; Rohmer, M. *Angew. Chem. Int. Ed.* **2002**, *41*, 4337-4339.
- (20) Itoh, T.; Nagano, T.; Sato, M.; Hirobe, M. *Tetrahedron Lett.* **1989**, *30*, 6387-6388.
- (21) Brandt, W.; Dessoy, M. A.; Fulhorst, M.; Gao, W.; Zenk, M. H.; Wessjohann, L.A. *ChemBioChem* **2004**, *5*, 311-323.
- (22) Grawert, T.; Kaiser, J.; Zepeck, F.; Laupitz, R.; Hecht, S.; Amslinger, S.; Schramek, N.; Schleicher, E.; Weber, S.; Haslbeck, M.; Buchner, J.; Rieder, C.; Arigoni, D.; Bacher, A.; Eisenreich, W.; Rohdich, F. *J. Am. Chem. Soc.* **2004**, *126*, 12847-12855.
- (23) Sweeney, A. M.; Lange, R.; Fernandes, R. P. M.; Schulz, H.; Dale, G. E.; Douangamath, A.; Proteau, P. J.; Oefner, C. *J. Mol. Biol.* **2005**, *345*, 115-127.
- (24) Eisenreich, W.; Schwarz, M.; Cartayrade, A.; Arigoni, D.; Zenk, M. H.; Bacher, A. *Chem. Biol.* **1998**, *5*, R221-R233.